ELASTOPLASTIC ANALYSIS OF ROTATING SHRINK-FITTED DISCS WITH NONLINEAR HARDENING CHARACTERISTICS

M. M. MEGAHED

Department of Mechanical Design and Production, Cairo University, Giza, Egypt

and

M. S. ABDEL-KADER

Department of Mechanical Engineering, Military Technical College, Cairo, Egypt

Abstract—Elastoplastic analysis of a thin rotating disc shrink-fitted to an elastic shaft is provided. A nonlinear hardening material with equivalent stress $\bar{\sigma} = Y + A(\bar{\varepsilon}_p)^n$, where A and n are constants, Y is the yield strength, and $\bar{\varepsilon}_p$ is the equivalent plastic strain, is employed. Tresca yield criterion is adopted, and the operating conditions (interference and rotation) are assumed to induce radial and hoop stresses which lie in the second quadrant of the Tresca hexagon. Quasi-analytical solutions are deduced for the radial distributions of plastic hoop strain as well as radial and hoop stresses for $n = 1, 1/2, 1/3$ and $1/4$. Validity domains of the solutions developed are determined and favourably compared to those of other investigators. Conditions for elastic shakedown limit are also discussed. In addition, an approximate solution is developed, which can be advantageously employed in the range $0 < n \leqslant 1$. Accuracy of the approximate solution in comparison with corresponding exact solutions is examined and found to be fairly good. Significance of results obtained as an aid to designers of shrink-fitted assemblies is also discussed.

INTRODUCTION

Shrink fits are widely used in mechanical constructions since they are capable of transmitting high torques at low production cost. The elastic design of a shrink-fitted disc is traditionally based upon Lamé's solution of thick-walled tubes. However, a purely elastic design does not fully utilize the strength of the disc. Hence, the concept of elastoplastic design is employed to overcome this shortcoming. Lundberg (1944) treated a nonrotating shrink fit assuming elastic–perfectly plastic material behaviour which follows the von Mises yield criterion. The resulting solution is employed in the German standards DIN 7190, via a large number of design charts. In order to provide solutions simpler than those by Lundberg, Kollmann (1978, 1981, 1984) treated shrink fits, both at rest and rotating, using the same basic assumptions as Lundberg, but employing Tresca's yield criterion instead of von Mises'. This procedure yielded relatively simpler design formulae.

Both Lundberg's and Kollmann's solutions neglect strain hardening of the disc material. Gamer (1986, 1987) considered a disc material with elastic linear strain hardening behaviour and obtained analytical expressions for stresses and strains in a rotating shrink-fit assuming Tresca's yield criterion.

In this paper, elastoplastic analysis of rotating shrink fits is provided for a general nonlinear hardening material. The material law employed is: $\bar{\sigma} = Y + A(\bar{\varepsilon}_p)^n$, where $\bar{\sigma}, \bar{\varepsilon}_p$ are the effective stress and plastic strain, respectively, Y is an initial yield stress and A, n are material constants characterizing the state of hardening with $0 < n \leqslant 1$, and $n = 1$ corresponding to linear hardening. Perfect plasticity corresponds to $A = 0$, and purely elastic behaviour to $A \to \infty$. The formulation of the problem is similar to the procedures followed by Megahed (1990, 1991), in which thick tubes and spheres under internal pressure are treated. This method of analysis has recently been adopted by Gamer (1991) to obtain general quasi-analytical solutions of elastoplastic problems with spherical and cylindrical symmetry and nonlinear hardening characteristics.

In common with previous investigations (Kollmann, 1981; Gamer, 1986, 1987), a solid elastic shaft is considered herein and the elastic moduli E, Poisson's ratios v and densities ρ are assumed to be equal for both shaft and disc. Furthermore, a state of plane stress is considered in both shaft and disc.

PROBLEM FORMULATION

Consider a thin flat disc, with inner radius a and outer radius b, shrunk onto a solid shaft of outer radius $a+\delta$. The disc has a free outer boundary. The shaft-disc assembly rotates with angular speed ω. The problem configuration is illustrated in Fig. 1, but prior to assemblage. The stress components are σ_θ, σ_r, σ_z $(= 0)$, and strain components are ε_r, ε_θ and ε_z. It is assumed that the loading conditions δ and ω are chosen such that $\sigma_\theta \geqslant 0$ and $\sigma_r \leqslant 0$, i.e. the stress state lies in the second quadrant of stress space, where the Tresca effective stress $\bar{\sigma} = \sigma_\theta - \sigma_r$. Total strains are decomposed into elastic and plastic components. Strain–displacement–stress relations in the disc are:

$$\varepsilon_r = \frac{\mathrm{d}u}{\mathrm{d}r} = \frac{1}{E}[\sigma_r - v\sigma_\theta] + \varepsilon_r^p, \tag{1a}$$

$$\varepsilon_\theta = \frac{u}{r} = \frac{1}{E}[\sigma_\theta - v\sigma_r] + \varepsilon_\theta^p, \tag{1b}$$

where u is the radial displacement. For the Tresca yield criterion and the associated flow rule, incompressibility of plastic strains requires that $\varepsilon_\theta^p/\varepsilon_r^p = -1$ and $\varepsilon_z^p = 0$. The equivalence of plastic work $(\sigma_{ij}\varepsilon_{ij}^p = \bar{\sigma}\bar{\varepsilon}_p)$ yields $\bar{\varepsilon}_p = \varepsilon_\theta^p = -\varepsilon_r^p$.

Inversion of eqn (1) yields stresses in terms of total and plastic strains as:

$$\sigma_r = \frac{E}{1-v^2}\left[\frac{\mathrm{d}u}{\mathrm{d}r} + v\frac{u}{r} + (1-v)\varepsilon_\theta^p\right], \tag{2a}$$

$$\sigma_\theta = \frac{E}{1-v^2}\left[\frac{u}{r} + v\frac{\mathrm{d}u}{\mathrm{d}r} - (1-v)\varepsilon_\theta^p\right]. \tag{2b}$$

The equilibrium condition in the radial direction is:

$$\frac{\mathrm{d}\sigma_r}{\mathrm{d}r} + \frac{\sigma_r - \sigma_\theta}{r} + \rho\omega^2 r = 0. \tag{3}$$

Substitution of eqns (2) into eqn (3) yields the following differential equation:

$$\frac{\mathrm{d}^2u}{\mathrm{d}r^2} + \frac{1}{r}\frac{\mathrm{d}u}{\mathrm{d}r} - \frac{u}{r^2} = -(1-v)\left[\frac{\mathrm{d}\varepsilon_\theta^p}{\mathrm{d}r} + 2\frac{\varepsilon_\theta^p}{r} + \frac{\rho(1-v)}{8E}\omega^2 r\right], \tag{4}$$

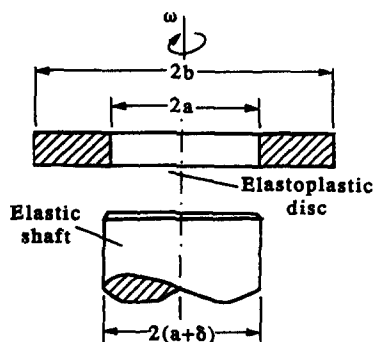whose solution can be readily obtained by double integration. After some manipulations,

Fig. 1. Rotating shrink-fit configuration prior to assemblage.

radial distributions of σ_r, σ_θ and u in the disc are obtained as:

$$\sigma_r = \frac{EA}{1-v} - \frac{BE}{1+v}\frac{1}{r^2} - \frac{3+v}{8}\rho\omega^2 r^2 - E\int_a^r \frac{\varepsilon_\theta^p}{r}\,dr, \tag{5a}$$

$$\sigma_\theta = \sigma_r + \frac{2BE}{1+v}\frac{1}{r^2} + \frac{1-v}{4}\rho\omega^2 r^2 - E\varepsilon_\theta^p, \tag{5b}$$

$$u = \frac{(1-v)r}{E}[\sigma_r + \tfrac{1}{4}\rho\omega^2 r^2] + \frac{2B}{1+v}\frac{1}{r}, \tag{5c}$$

where A, B are integration constants.

Considering the elastic shaft, and following the same procedure as above, yields the following radial distributions of σ_r, σ_θ and u for $0 \leqslant r \leqslant a$:

$$\sigma_r = \frac{EC}{1-v} - \frac{DE}{1+v}\frac{1}{r^2} - \frac{3+v}{8}\rho\omega^2 r^2, \tag{6a}$$

$$\sigma_\theta = \sigma_r + \frac{2DE}{1+v}\frac{1}{r^2} + \frac{1-v}{4}\rho\omega^2 r^2, \tag{6b}$$

$$u = \frac{(1-v)}{E}r[\sigma_r + \tfrac{1}{4}\rho\omega^2 r^2] + \frac{2D}{1+v}\frac{1}{r}, \tag{6c}$$

where C and D are integration constants.

The boundary conditions necessary to determine the constants A, B, C and D are:

(1) $u = 0$ at $r = 0$,
(2) $\sigma_r (r = a)$ for the disc $= \sigma_r (r = a)$ for the shaft,
(3) $\sigma_r = 0$ at $r = b$,
(4) $\delta = u (r = a)$ for the disc $- u(r = a)$ for the shaft.

Applying the above conditions yields the following:

$$\frac{EA}{1-v} = \frac{E\delta a}{2b^2} + \frac{3+v}{8}\rho\omega^2 b^2 + E\int_a^c \frac{\varepsilon_\theta^p}{r}\,dr, \tag{7a}$$

$$\frac{EB}{1+v} = \frac{E\delta a}{2}, \tag{7b}$$

$$\frac{EC}{1-v} = \frac{EA}{1-v} - \frac{EB}{1+v}\frac{1}{a^2}, \tag{7c}$$

$$D = 0, \tag{7d}$$

where c is the radius of the elastic plastic front, and $a \leqslant c \leqslant b$.

Hence, the final expressions for σ_r, σ_θ and u in the disc are obtained as:

$$\sigma_r/Y = \frac{\Delta}{2}(Z_0 - Z) + \Omega^2(1 - Z_0/Z) + (I - \bar{I}), \tag{8a}$$

$$\sigma_\theta/Y = \sigma_r/Y + Z\Delta + \hat{\Omega}^2/Z - \psi, \tag{8b}$$

$$u = \frac{1-v}{E}r[\sigma_r + \tfrac{1}{4}\rho\omega^2 r^2], \tag{8c}$$

where

$$\psi = \frac{E\varepsilon_\theta^p}{Y} \tag{9}$$

is a normalized plastic hoop strain,

$$Z = a^2/r^2, \qquad Z_0 = a^2/b^2, \qquad \bar{Z} = a^2/c^2. \tag{10a, b, c}$$

Note that $Z = 1$ at the shaft-disc interface $r = a$. The integrals I and $\bar{I}$ are given accordingly by:

$$I = \frac{1}{2} \int_1^Z \frac{\psi}{Z} \, dZ, \qquad \bar{I} = \frac{1}{2} \int_1^{\bar{Z}} \frac{\psi}{Z} \, dZ, \tag{11a, b}$$

and

$$\Delta = \frac{E\delta}{aY}, \qquad \Omega^2 = \tfrac{1}{8}(3+v)\rho\omega^2 b^2/Y, \tag{12a, b}$$

$$\hat{\Omega}^2 = \frac{2(1-v)}{3+v} Z_0 \Omega^2, \tag{12c}$$

are dimensionless measures of shrink fit and centrifugal forces due to rotation, respectively.

At the elastoplastic front $r = c$, the effective stress $\bar{\sigma} = \sigma_\theta - \sigma_r = Y$ and $\psi = 0$. Hence, from eqn (8b) the plastic front is related to applied loads by:

$$\bar{Z}^2 - \bar{Z}/\Delta + \hat{\Omega}^2/\Delta = 0. \tag{13}$$

Solution of the quadratic equation (13) yields:

$$\bar{Z} = \frac{1}{2\Delta} \pm \frac{1}{2\Delta} \sqrt{1 - 4\hat{\Omega}^2\Delta}. \tag{14a}$$

The positive sign should be used so that the plastic front radius $c = a/\sqrt{\bar{Z}}$ increases with rotation. For nonrotating shrink-fits ($\hat{\Omega}^2 = 0$), eqn (14a) reduces to

$$\bar{Z} = \frac{1}{\Delta}. \tag{14b}$$

Note that eqn (14a) yields the elastoplastic front for any combination of Δ and Ω^2, and is obtained without specifying any hardening law for the disc material. Moreover, for the above solution to be valid, the discriminant $(1 - 4\hat{\Omega}^2\Delta)$ should be non-negative, i.e.

$$4\hat{\Omega}^2\Delta \leqslant 1, \tag{15}$$

which represents the portion of the $\hat{\Omega}^2$ versus Δ space under the hyperbola $4\hat{\Omega}^2\Delta = 1$. This condition will be further examined later.

HARDENING LAW

A general nonlinear hardening law that has proved to be most relevant in the analysis of small strain plasticity problems is:

$$\bar{\sigma} = Y + A(\bar{\varepsilon}_p)^n, \tag{16}$$

where A and n are material constants. This particular hardening law is preferred to other nonlinear hardening representations such as the Ramborg–Osgood law ($\bar{\varepsilon} = \bar{\sigma}/E + (\bar{\sigma}/K)^{1/m}$) due to its consistency with the observed smooth transition between elastic and plastic states. In addition, the above hardening law allows analytical treatment of an important class of

elastoplastic problems as illustrated by Megahed (1990, 1991), Megahed and Abbas (1991) and Abol-Liel *et al.* (1992). Equation (16) can be rewritten as:

$$\bar{\sigma} = Y[1 + H\psi^n],\tag{17a}$$

where H is a hardening parameter defined as:

$$H = \frac{A}{Y}(Y/E)^n.\tag{17b}$$

A physical interpretation of the hardening parameter H is that it represents the rise in flow stress at $\psi = 1$ above the initial yield value Y. Note that $\psi = 1$ corresponds to $\bar{\varepsilon}_p = Y/E$, i.e. the elastic strain at yield.

Values of H and n have been collected by Megahed (1991) and Rees (1987a, b) who both concluded that n ranges from 0.1 to about 0.7, with $n = 1/3$ as characteristic of many engineering alloys. The value of H was found to be always less than unity and often less than 0.5 for the majority of engineering alloys. Clearly, perfect plasticity corresponds to $H = 0$ and purely elastic behaviour to $H \to \infty$.

ANALYTICAL SOLUTION FOR PLASTIC HOOP STRAIN

The effective Tresca stress $\bar{\sigma} = \sigma_\theta - \sigma_r$ can be obtained from eqns (8a, b) as:

$$\bar{\sigma}/Y = Z\Delta + \hat{\Omega}^2/Z - \psi.\tag{18}$$

Comparison between expressions of $\bar{\sigma}$ obtained from eqns (17a) and (18) yields:

$$H\psi^n + \psi = Z\Delta + \hat{\Omega}^2/Z - 1.\tag{19a}$$

The right-hand side of eqn (19a) is a function of radial position Z and the loading parameters Δ and $\hat{\Omega}^2$. The expression $Z\Delta + \hat{\Omega}^2/Z - 1$ is denoted by $F(Z)$. Therefore, eqn (19a) is written simply as:

$$H\psi^n + \psi = F.\tag{19b}$$

Clearly, $F(Z) > 0$ within the elastoplastic zone since $\psi > 0$ for $\bar{Z} < Z \leqslant 1$, and $F(Z) = 0$ within the outer elastic zone $(Z_0 < Z < \bar{Z})$. For perfectly plastic behaviour, $H = 0$ and ψ is obtained from eqn (19a) as: $\psi = Z\Delta + \hat{\Omega}^2/Z - 1$.

The above nonlinear equation can be solved analytically for $n = 1, 1/2, 1/3$ and $1/4$ as reported by Megahed (1990, 1991). Radial distributions of ψ corresponding to the above four values of n are given in Table 1.

Table 1. Analytical solutions for normalized hoop strain ψ

n	Distribution of ψ, $F = \Delta Z + \hat{\Omega}^2/Z - 1$	Eqn no.
1	$\psi = F/(H+1)$	(20)
1/2	$\psi = F + \dfrac{H^2}{2} - \dfrac{H^2}{2}\sqrt{1 + 4F/H^2}$	(21)
1/3	$\psi = F + H[\tfrac{1}{2}\sqrt{4H^3/27 + F^2} - F/2]^{1/3} - H[\tfrac{1}{2}\sqrt{4H^3/27 + F^2} + F/2]^{1/3}$	(22)
1/4	$\psi = F + K - K\sqrt{\tfrac{1}{4}H^4/K^3 - 1}$	(23a)
where	$K^2 = \dfrac{H^2}{2}[\sqrt{(F/3)^3 + (H/4)^4} + (H/4)^2]^{1/3} - \dfrac{H^2}{2}[\sqrt{(F/3)^3 + (H/4)^4} - (H/4)^2]^{1/3}$	(23b)

The integral $I = \frac{1}{2}\int_1^Z \psi/Z \, dZ$ appearing in eqn (8a) can be evaluated analytically for the case of linear hardening $n = 1$ only. For $n \neq 1$, resort is made to numerical integration. For the case of linear hardening ($n = 1$), the expression for the integral I is:

$$I = \frac{1}{2(H+1)}[(Z-1)\Delta + \hat{\Omega}^2(1 - 1/Z) - \ln Z].$$ (24)

$\bar{I}$ is obtained by substituting $\bar{Z}$ from eqn (14a) into eqn (24). Once I and $\bar{I}$ are determined, stresses can be readily calculated from eqns (8a, b). In the elastic region ($c \leqslant r \leqslant b$), note that $I = \bar{I}$ and $\psi = 0$.

The procedure employed in the above analysis assumes a rather hypothetical sequence of loading in which both interference (Δ) and rotation (Ω^2) loads are applied simultaneously and proportionally. In practice, the disc is first shrunk to the shaft and rotation is applied subsequently. It can be easily shown that as long as the stress states in the elastoplastic zone are confined to the second quadrant of the Tresca hexagon ($\bar{\sigma} = \sigma_\theta - \sigma_r$, $\varepsilon_\theta^p/\varepsilon_r^p = -1$), the final states of stress and plastic strain are the same for the above two sequences of loading. The conditions required for the above limitation to be satisfied are discussed subsequently.

RANGE OF VALIDITY

In order to use the above results correctly, their range of validity has to be determined in terms of the two loading parameters Δ and Ω^2. To generate the required ranges it is necessary to determine the conditions for:

(1) Transition from fully elastic behaviour to partially plastic behaviour. This occurs when $\bar{Z} = 1$.
(2) Transition from partially plastic behaviour to fully plastic behaviour. This occurs when $\bar{Z} = Z_0$.
(3) Within the ranges set out by the above two conditions, the state of stress at any point lying within $\bar{Z} < Z < 1$ must be in the second quadrant of the Tresca hexagon, where $\bar{\sigma}$ is equal to $\sigma_\theta - \sigma_r$ and $\bar{\varepsilon}_p$ to ε_θ^p.

Substituting $\bar{Z} = 1$ into eqn (14a) and using eqn (12) yield:

$$\Omega^2 \geqslant \frac{3+v}{2(1-v)} \frac{(1-\Delta)}{Z_0}.$$ (25)

Hence, the condition for transition from purely elastic to elastoplastic behaviour occurs when the equality sign holds in (25), as shown in Fig. 2 for a disc with $b/a = 2$. Note that for a nonrotating shrink fit ($\Omega^2 = 0$), the above transition occurs when $\Delta = 1$. Fully elastic behaviour is obtained for values of Ω^2 violating eqn (25). For a purely elastic rotating shrink-fit, interference between shaft and disc is lost when $\sigma_r(r = a)$ becomes equal to zero. It can be easily shown that the lost interference condition reads

$$\Omega^2 = \Delta/2.$$ (26)

Hence, for values of Ω^2 greater than $\Delta/2$, the shrink-fit is incapable of transmitting any torque.

It is interesting to note that the two lines specified by eqns (25), (26) intersect at:

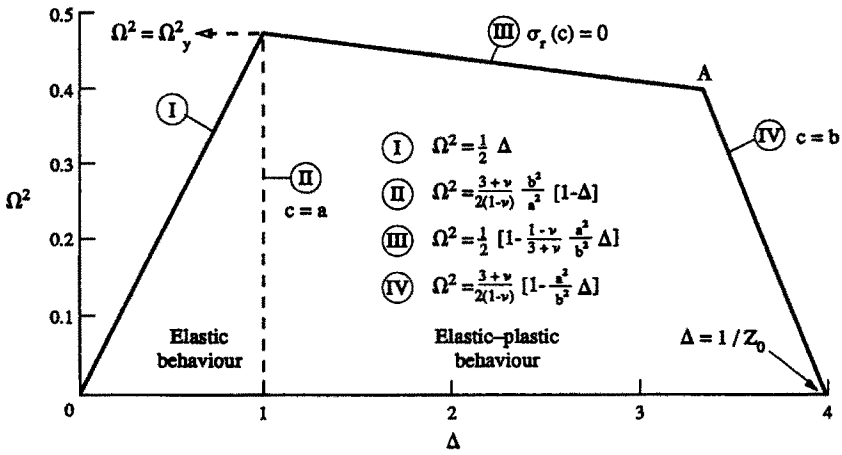$$\Omega^2 = \frac{1}{2} \frac{1}{1 + \dfrac{1-v}{3+v} Z_0},$$ (27)

Fig. 2. Validity domain for a disc with $b/a = 2$.

which is exactly the same value as Ω_y^2 causing initial yield in a freely rotating annular disc (Benham and Crawford, 1988).

Combinations of Ω^2 and Δ to the right of the line specified by equality (25) induce partial plastification in the disc. Fully plastic disc is obtained when the plastic front $c = b$, i.e. $\bar{Z} = Z_0$ in eqn (14a), which yields:

$$\Omega^2 = \frac{3+v}{2(1-v)}(1 - Z_0\Delta). \tag{28}$$

Note that for a nonrotating shrink-fit ($\Omega^2 = 0$) the value of Δ causing full disc plastification is $\Delta = 1/Z_0$.

Within the partial plasticization region lying between the two lines specified by eqns (25) and (28), the proposed formulation is correct provided the loading points remain within the second quadrant of the Tresca hexagon, Fig. 3, in which $\bar{\sigma} = \sigma_\theta - \sigma_r$, $\sigma_\theta > 0$ and $\sigma_r < 0$ for $a < r < c$. Inspection of radial distributions of σ_r and σ_θ within the elasto-plastic zone shows that the corresponding sufficient conditions are: $\sigma_r(r = c) \leqslant 0$ and $\sigma_\theta(r = a) > 0$. The condition $\sigma_r(r = c) \leqslant 0$ can be evaluated irrespective of the hardening characteristics of the material. From eqn (8a), it can be seen that $\sigma_r(r = c) \leqslant 0$, when

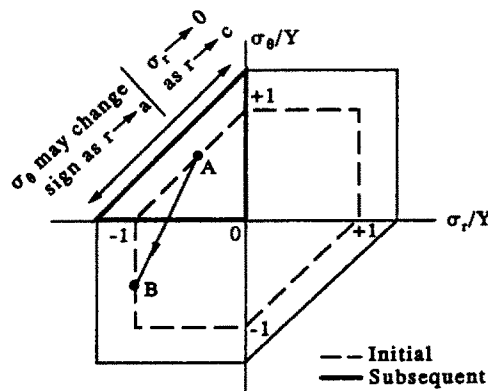$$\Omega^2 \leqslant \frac{\Delta}{2}\bar{Z}, \tag{29}$$

Fig. 3. Admissible stress domain.

which, upon using eqn (14a), reduces to

$$\Omega^2 \leqslant \frac{1}{2}\left(1 - \frac{1-\nu}{3+\nu} Z_0 \Delta\right). \tag{30}$$

It is worth noting that the line described by equality (30) intersects the two lines obtained from equality (25) and eqn (26) at $\Omega^2 = \Omega_y^2$.

The condition of $\sigma_\theta(r = a) \geqslant 0$ can be evaluated analytically for the cases of perfect plasticity and linear hardening. For perfect plasticity $(H = 0)$, eqn (20) yields $\psi = Z\Delta + (\hat{\Omega}^2/Z) - 1$, whereas eqn (11b) gives

$$\bar{I} = \frac{1}{2}\left[\hat{\Omega}^2\left(1 - \frac{1}{\bar{Z}}\right) - \Delta(1 - \bar{Z}) - \ln \bar{Z}\right].$$

At $r = a$ $(Z = 1)$, $I = 0$ and σ_r can be obtained from eqn (8a) and then substituted into eqn (8b) to give the condition

$$\sigma_\theta(r = a)/Y = \left(\Omega^2 - \frac{\Delta}{2}\right)(1 - Z_0) + \frac{\Delta}{2}(1 - \bar{Z}) - \frac{\hat{\Omega}^2}{2}\left(1 - \frac{1}{\bar{Z}}\right) + \tfrac{1}{2}\ln \bar{Z} + 1 \geqslant 0. \tag{31}$$

Substituting for $\hat{\Omega}^2$ from (12c) and $\bar{Z}$ from eqn (14a), a nonlinear relation between Δ and Ω^2 is readily obtained. Condition (31) represents a new limitation to the validity domain, as shown in Fig. 4 for a disc with $b/a = 4$. It is obvious that the validity domain has been considerably reduced upon imposing the condition $\sigma_\theta(r = a) \geqslant 0$. For a nonrotating shrink-fit $(\Omega^2 = 0, \bar{Z} = 1/\Delta)$, the above equality reduces to $Z_0\Delta + 1 = \ln \Delta$, which, for the case of Fig. 4 $(Z_0 = a^2/b^2 = 1/16)$, yields $\Delta = 3.35$. Note that the condition $\sigma_\theta(r = a) > 0$ is satisfied at all points of the validity domain of Fig. 2, for which $b/a = 2$.

Similarly, for linear hardening $(n = 1, H \neq 0)$, the condition that $\sigma_\theta(r = a) \geqslant 0$ reads

$$\sigma_\theta(r = a)/Y = \left(\Omega^2 - \frac{\Delta}{2}\right)(1 - Z_0) + \frac{1}{2(H+1)}\left[(1 - \bar{Z})\Delta - \hat{\Omega}^2\left(1 - \frac{1}{\bar{Z}}\right) + \ln \bar{Z}\right]$$

$$+ \frac{1}{H+1}(H\Delta + \hat{\Omega}^2 H + 1) \geqslant 0, \tag{32}$$

which is seen to reduce to condition (31) for $H = 0$. For other values of n, however, this condition may be checked only after numerical evaluation of the integrals I and $\bar{I}$. Note
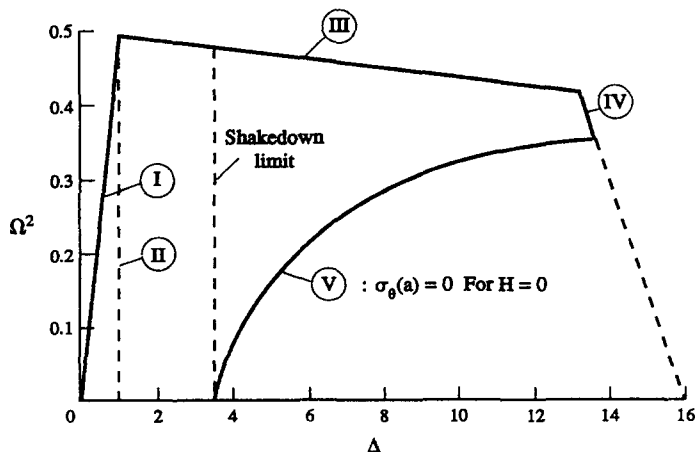

Fig. 4. Validity domain for a disc with $b/a = 4$.

that Gamer (1986) did not take this condition into account when constructing the domain of validity.

Simple calculations can show that the condition prescribed by eqn (15) does not represent a new limitation to the validity domain developed above since the hyperbola $\hat{\Omega}^2\Delta = 1/4$ can be shown not to intersect the validity domain at any point. This may be easily checked by substituting the coordinates of the most distant point from the origin (e.g. point A of Fig. 2) into eqn (15), i.e.

$$\Delta = \frac{3+v}{4Z_0} \quad \text{and} \quad \Omega^2 = \frac{3+v}{8},$$

thus providing $v^2 + 2v + 1 \geqslant 0$, which is always satisfied.

ELASTIC UNLOADING

The shaft-disc assembly will be subjected to consecutive rotation-stand still cycles during its operation and therefore investigation of the unloading behaviour becomes important to designers. Of particular interest is the condition of elastic shakedown, which guarantees that no further plastic deformation is developed during unloading–reloading cycles subsequent to initial loading. Determination of the shakedown limit depends upon the changes which take place in the size, shape and centre coordinates of the yield surface as a result of plastic deformation induced during initial loading. These changes may be modelled by isotropic hardening (Hill, 1950), kinematic hardening (Prager, 1956) or suitable combinations of both rules. A full analysis of the unloading behaviour taking into account the changes in the yield surface is beyond the scope of the present work. Shakedown is analysed here assuming a perfectly plastic material behaviour ($H = 0$).

Consider a disc operating in the elastoplastic regime under prescribed values of Δ and Ω^2 lying within the validity region discussed earlier. These operating conditions induce a stress state such as that indicated by point A illustrated on the Tresca hexagon shown in Fig. 3. Reduction of the speed of rotation to zero and assuming elastic unloading poses a disc-shaft assembly problem which can be treated in a manner similar to that of the loading problem—but a lot simpler—to yield the following distribution of changes in radial and hoop stresses:

$$\Delta\sigma_r/Y = -\Omega^2(1 - Z_0/Z), \tag{33a}$$

$$\Delta\sigma_\theta/Y = \Delta\sigma_r/Y - \hat{\Omega}^2/Z. \tag{33b}$$

Note that both $\Delta\sigma_r$ and $\Delta\sigma_\theta$ are negative and that the slope of the elastic unloading path is always greater than unity. Hence, unloading takes place along paths similar to the line indicated by AB in Fig. 3. Consider the most severely stressed point in the disc, i.e. at $r = a$ ($Z = 1$). The corresponding condition of pure elastic unloading is:

$$\sigma_r^{(0)}(Z = 1) + \Delta\sigma_r(Z = 1) < -Y, \tag{34}$$

where $\sigma_r^{(0)}(Z = 1)$ refers to the radial stress following the loading phase. For perfectly plastic behaviour, $\sigma_r^{(0)}(Z = 1)$ can be expressed in terms of Δ and Ω^2 by substitution from eqns (14a) and (24) into eqn (8a). After some manipulations, the shakedown condition is obtained as:

$$\Delta \leqslant \tfrac{1}{2}[1 + \sqrt{1 - 4\hat{\Omega}^2\Delta}] \cdot \exp[2 + Z_0\Delta - \hat{\Omega}^2 - \sqrt{1 - 4\hat{\Omega}^2\Delta}]. \tag{35}$$

GENERAL APPROXIMATE SOLUTION

An approximate solution can be obtained for the distribution of plastic hoop strain which is valid for any value of $0 < n < 1$. For $H < 1$, the nonlinear term $H\psi^n$ in eqn (19)

can be neglected and a first approximation for ψ is $\psi \simeq Z\Delta + \hat{\Omega}^2/Z - 1$, which is the perfect plasticity solution. Back substitution of this first approximation into the nonlinear term $H\psi^n$ of eqn (19) yields:

$$\psi \simeq (Z\Delta + \hat{\Omega}^2/Z - 1) - H(Z\Delta + \hat{\Omega}^2/Z - 1)^n. \tag{36}$$

The second term represents the inhibition of plastic strain due to hardening, while the first term is the perfect plasticity solution. Inspection of eqn (36) indicates that the normalized hoop strain $\psi = 0$ at two values of Z; when $Z\Delta + \hat{\Omega}^2/Z - 1 = 0$, i.e. at $Z = \bar{Z}$, and also at $Z = Z^*$, where

$$Z^*\Delta + \hat{\Omega}^2/Z^* - 1 = H^{1/(1-n)}, \tag{37a}$$

which yields

$$Z^* = \frac{1 + H^{1/(1-n)}}{2\Delta} + \frac{1 + H^{1/(1-n)}}{2\Delta}\sqrt{1 - 4\frac{\hat{\Omega}^2\Delta}{(1 + H^{1/(1-n)})^2}}. \tag{37b}$$

It can be shown that $1 > Z^* > \bar{Z}$, which means that the proposed approximate solution yields negative plastic hoop strain in the zone $\bar{Z} < Z < Z^*$. This error in the approximate solution appears to be greater near the plastic front when plastic strain is quite small. Since negative strains cannot be permitted, an exact statement of the approximate solution becomes:

$$\psi = (Z\Delta + \hat{\Omega}^2/Z - 1) - H(Z\Delta + \hat{\Omega}^2/Z - 1)^n, \quad Z^* < Z < 1, \tag{38a}$$

$$\psi = 0, \quad \bar{Z} < Z < Z^*. \tag{38b}$$

NUMERICAL RESULTS AND DISCUSSION

Figure 5 depicts the exact and approximate distributions of: (a) radial and hoop stresses and (b) plastic hoop strain as function of radial distance for a linear hardening ($n = 1$, $H = 0.2$), shrink-fitted rotating disc with $b/a = 2$ and the operating conditions $\Omega^2 = 0.4$ and $\Delta = 3.0$. It is clear from Fig. 5(a) that the hoop stress is positive and increases in the plastic zone ($a \leqslant r \leqslant c$) and decreases in the elastic zone ($c \leqslant r \leqslant b$). The radial stress is negative and approaches zero at the outer boundary $r = b$. When $\Omega^2 = 0$, i.e. a non-rotating shrink-fitted disc, both stresses maintain the same distributions, though at lower magnitudes. It is also clear from Fig. 5(b) that rotation has the effect of increasing the radius of the plastic zone. The plastic hoop strain is seen to be highest at the inner boundary ($r = a$). Moreover, within the plastic zone ($a \leqslant r \leqslant c$), the plastic hoop strain in the rotating disc is higher than in the nonrotating disc.

Figure 5 also shows that the approximate solution is generally in fairly good agreement with the exact solution, except probably at the inner boundary ($r = a$), where discernible differences are seen particularly in hoop stress and plastic strain. These differences diminish with increasing r and eventually vanish as r approaches the plastic front. Note that for $n = 1$ and $H < 1$, the exact and approximate plastic front radii coincide, i.e. ($c \equiv a/\sqrt{\bar{Z}}) = (c^* \equiv a/\sqrt{Z^*})$, as may be checked from eqns (14a) and (37b). This is not the case, however, for other values of n, as will be shown subsequently.

Figure 6 shows the distributions of: (a) radial and hoop stresses and (b) plastic hoop strain in the radial direction for the same operating conditions of Fig. 5, but for a nonlinear hardening disc ($n = 1/2$, $H = 0.2$), $b/a = 2$ employing both exact and approximate solutions. The stresses and plastic hoop strain distributions are, in general, similar to those obtained for the linear-hardening disc. The exact and approximate solutions are still in fairly good agreement, although they differ from those of Fig. 5. Whereas the exact plastic front radius, eqn (14a), does not depend on the hardening characteristics (n, H) of the disc material, the approximate radius, eqn (37b), does depend on n and H and has a lower value
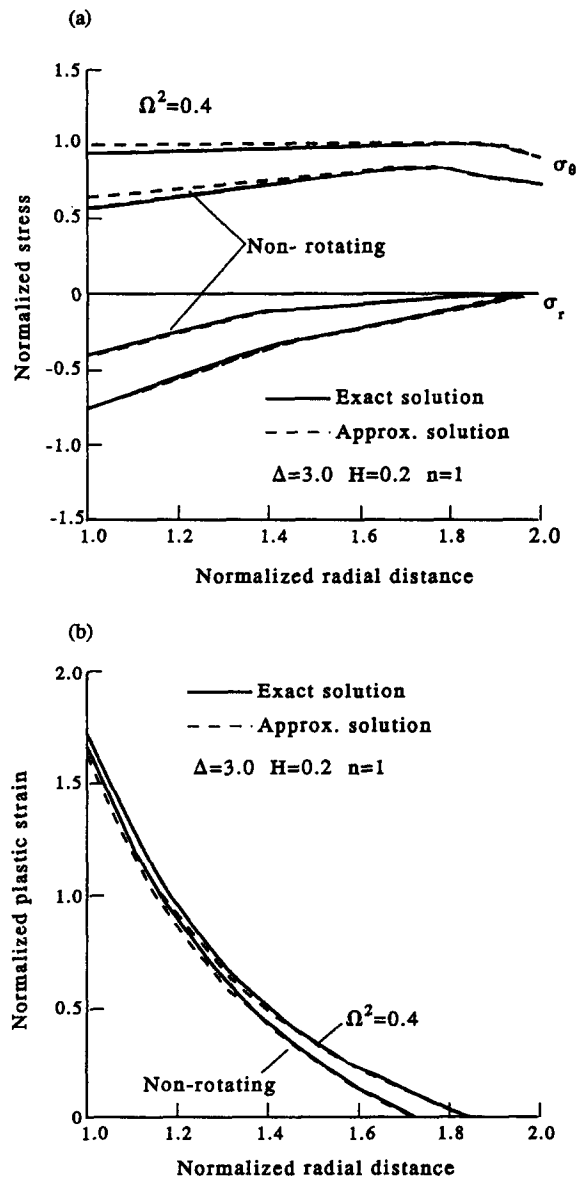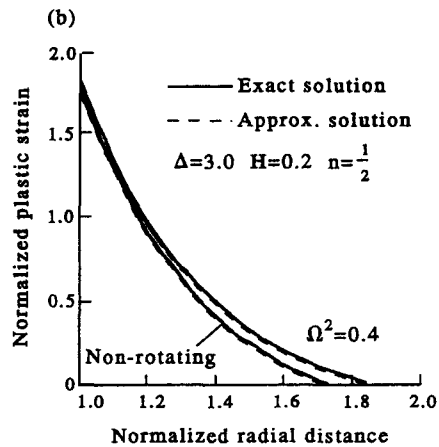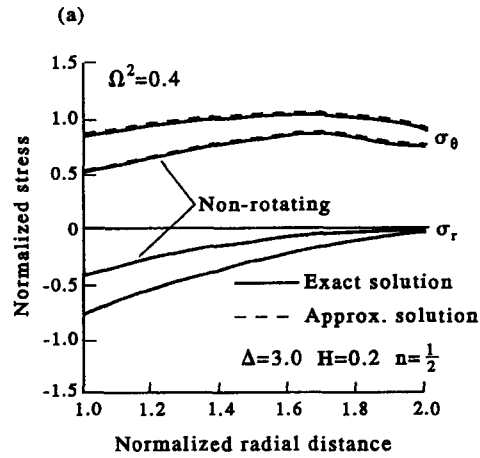
(a)

(b)

Fig. 5. Exact and approximate radial distribution of (a) radial and hoop stresses, and (b) plastic hoop strain for rotating and nonrotating discs with $b/a = 2, n = 1$.

$c^* \equiv a/\sqrt{Z^*}$. Effectively, the error in the approximate solution appears to be greater, yet acceptable, near the plastic front, particularly for the hoop stress and plastic strain.

Figures 7 and 8 depict the radial and hoop stresses and the plastic hoop strain for a nonlinear hardening disc with $n = 1/3$ and $n = 1/4$, respectively. Other operating conditions and material parameters have the same values used to produce Figs 5 and 6. The results are seen to be qualitatively similar to those of Fig. 6, but the errors near the plastic front seem to increase with decreasing n. At the inner boundary, however, where the stresses and strains assume their highest values, excellent agreement between the exact and approximate solutions is generally obtained.

A better understanding of the above comparisons between the exact and approximate solutions can be gained by critical examination of eqn (37b) identifying the approximate plastic front radius, Z^*. The value of Z^* approaches the exact value, $\bar{Z}$ of eqn (14a), as $H^{1/(1-n)}$ approaches zero. The contours of $H^{1/(1-n)}$ are illustrated in Fig. 9 in a plot of H versus n. It is clear that $H^{1/(1-n)} = 0$, for which $Z^* = \bar{Z}$, when $H = 0$ (perfect plasticity) or

Fig. 6. Exact and approximate radial distribution of (a) radial and hoop stresses, and (b) plastic hoop strain for rotating and nonrotating discs with $b/a = 2$, $n = 1/2$.
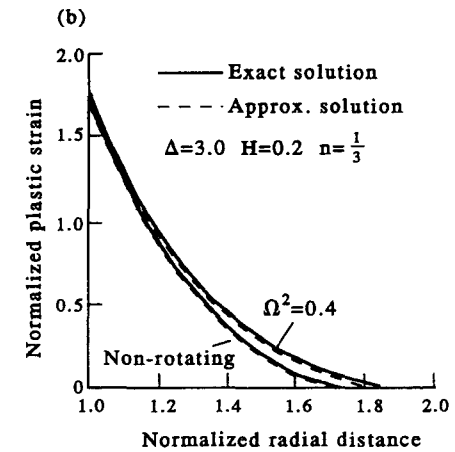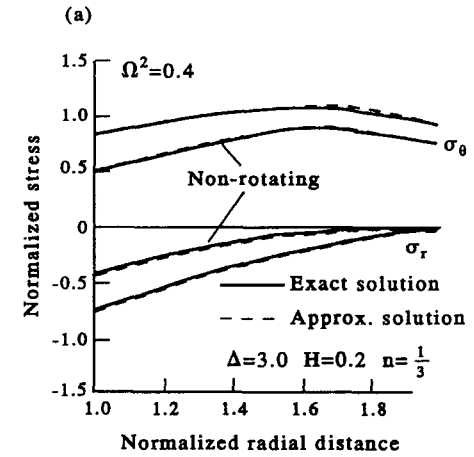

Fig. 7. Exact and approximate radial distribution of (a) radial and hoop stresses, and (b) plastic hoop strain for rotating and nonrotating discs with $b/a = 2$, $n = 1/3$.
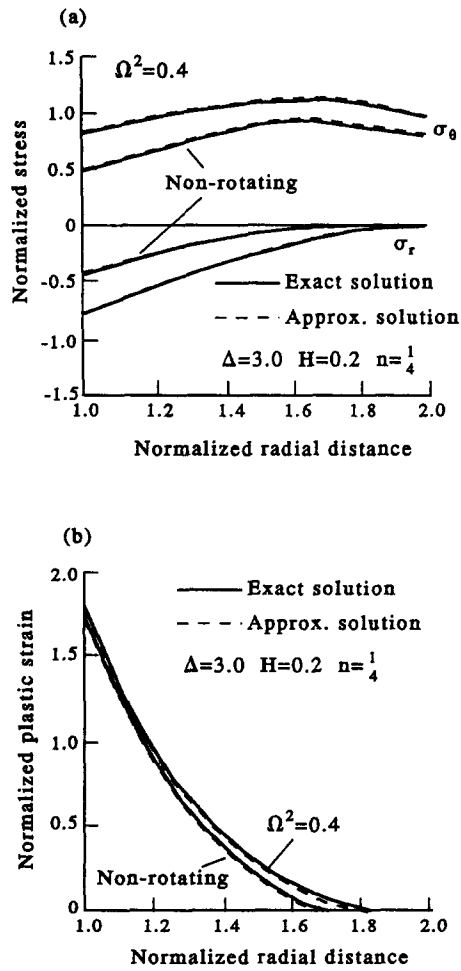
(a)

(b)

Fig. 8. Exact and approximate radial distribution of (a) radial and hoop stresses, and (b) plastic hoop strain for rotating and nonrotating disc with $b/a = 2$, $n = 1/4$.
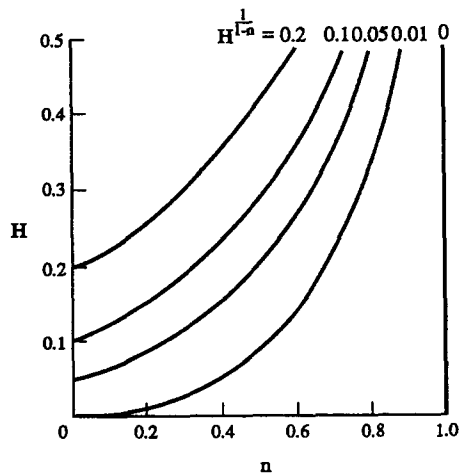

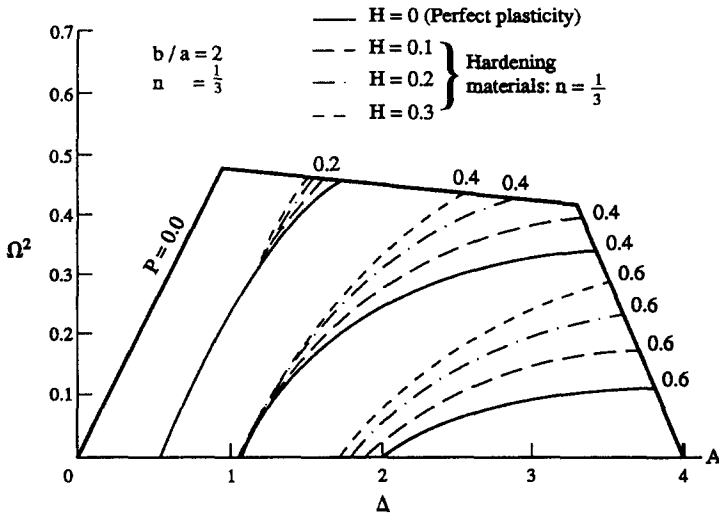Fig. 9. Contours of $H^{1/(1-n)}$ used to assess accuracy of the approximate solution.

Fig. 10. Effect of hardening parameter H on contours of interference pressure for a disc with $b/a = 2$.

$n = 1$ (linear hardening) (cf. Fig. 5 for the latter case). As H becomes larger and n becomes smaller, $H^{1/(1-n)}$ increases and Z^* begins to differ appreciably from $\bar{Z}$, as may be seen from Figs 6–8; as n changes from 1/2, Fig. 6, to 1/4, Fig. 8, the differences between the exact and approximate solutions become larger.

Figure 10 illustrates the contours of the normalized interference pressure $p = -\sigma_r(r = a)/Y$ as affected by the operating conditions (Ω^2, Δ) for a disc with $b/a = 2$. Obviously, such information is invaluable to designers, since it assists in determining the reduction in load-carrying capacity of a shrink-fit due to rotation a priori. The sensitivity of the pressure contours to changes in the hardening parameter H has also been studied, and the results are included in Fig. 10 for $H = 0$ (perfect plasticity), 0.1, 0.2, 0.3 and $n = 1/3$. As H increases, less reduction in interference pressure due to rotation is effected.

Figure 11 shows the contours of the interference pressure for a disc with $b/a = 3$ and $H = 0$ (perfect plasticity). Note the lowest contour $(P = 1)$, which implies that $\sigma_\theta(r = a) = 0$, eqn (31). As such, it represents again a limitation to the validity domain, since operating conditions below that contour represent stress states in the third quadrant of Tresca hexagon.

Figure 12 presents a similar set of results showing contours of P for a disc with $b/a = 4$ and $H = 0$. Sensitivity, to increasing values of the hardening parameter H, of the contours corresponding to the limitation $\sigma_\theta(r = a) = 0$ has also been investigated, and the results are
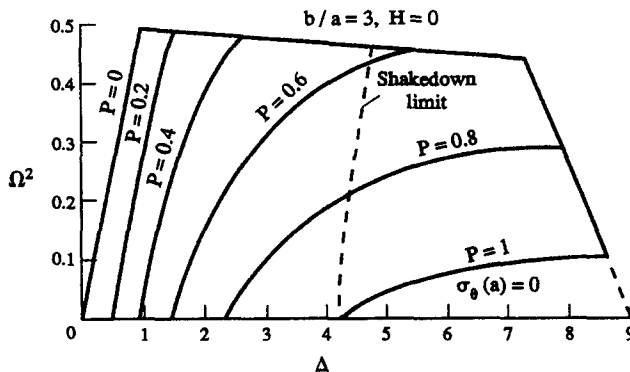

Fig. 11. Contours of interference pressure for a disc with $b/a = 3$, $H = 0$.
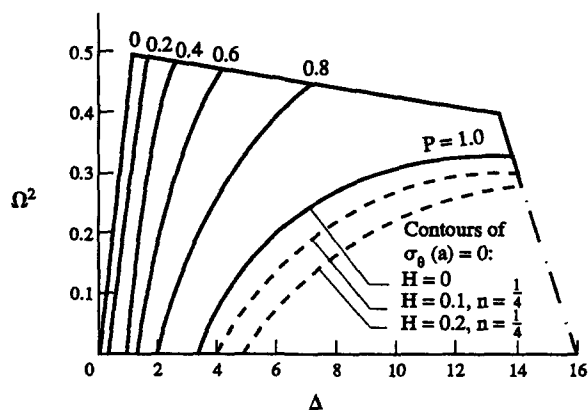
Fig. 12. Contours of interference pressure for a disc with $b/a = 4$.

shown in Fig. 12; as H increases, this limitation relaxes slightly, and the validity domain increases correspondingly. In obtaining the above results Δ, Ω^2, Z_0, H, n needed to be specified. In addition, $v = 0.3$ was assumed.

The shakedown condition has been numerically evaluated for discs with $b/a = 2, 3$ and 4. The results show that elastic shakedown behaviour encloses the whole validity region for $b/a = 2$, while for $b/a = 3$ and $b/a = 4$ shakedown regions constitute only part of the validity region, as shown in Figs 11, 4, respectively. It is observed that as b/a becomes larger the shakedown region occupies a smaller portion of the elastoplastic zone. This result is to be expected, since centrifugal stresses become more significant as the mass of the disc increases.

It is worth noting that the quasi-analytical solutions developed here were limited to four specific values of the material hardening exponent ($n = 1, 1/2, 1/3, 1/4$), whereas the approximate solution can be used advantageously in the range $0 < n \leqslant 1$. Cyclic behaviour of shrink-fitted assemblies operating beyond the elastic shakedown limit is an interesting problem which deserves further elaboration in a future work. Also, analysis of shrink-fitted discs, with von Mises yield criterion adopted, can be attempted. Resort to numerical methods is anticipated in this case.

REFERENCES

Abol-Liel, A. H., Abdel-Kader, M. S., Sallam, M. T. and Momeh, Z. Z. (1992). Characterization and modeling of the behaviour of a strain hardening material. *Fifth Appl. Mech. Engng Conf.*, M.T.C., Cairo, 5–7 May.

Benham, P. P. and Crawford, R. J. (1988). *Mechanics of Engineering Materials*. ELBS/Longman, London.

Gamer, U. (1986). The rotating elastic–plastic shrink fit with hardening. *Acta Mech.* **61**, 15–27.

Gamer, U. (1987). The shrink fit with elastic–plastic hub exhibiting constant yield stress followed by hardening. *Int. J. Solids Structures* **23**, 1219–1224.

Gamer, U. (1991). On the quasi-analytical solutions of elastic–plastic problems with nonlinear hardening. In *Advances in Continuum Mechanics* (Edited by O. Bruller, V. Mannl and J. Najar), pp. 168–177. Springer, Berlin.

Hill, R. (1950). *The Mathematical Theory of Plasticity*. Clarendon Press, Oxford.

Kollmann, F. G. (1978). Die Auslegung elastisch–plastisch beansprucher Querpreßerbande. *Forsch. Ing.-Wes.* **44**, 1–11.

Kollmann, F. G. (1981). Rotating elasto–plastic interference fits. *Trans. Am. Soc. Mech. Engrs, J. Mech. Des.* **103**, 16–66.

Kollmann, F. G. (1984). *Welle-Nabe-Verbindungen, Konstruktion-sbucher Bd. 32*. Springer, Berlin.

Lundberg, G. (1944). Die Festigkeit von Preßsitzen. *Kugellager* **19**, 1–11.

Megahed, M. M. (1990). Elastic–plastic behaviour of a thick-walled tube with general nonlinear hardening properties. *Int. J. Mech. Sci.* **32**, 551–563.

Megahed, M. M. (1991). Elastic–plastic behaviour of spherical shells with nonlinear hardening properties. *Int. J. Solids Structures* **27**, 1499–1514.

Megahed, M. M. and Abbas, A. T. (1991). Influence of reverse yielding on residual stresses induced by autofrettage. *Int. J. Mech. Sci.* **33**, 139–150.

Prager, W. (1956). The theory of plasticity: a survey of recent achievements. *Proc. Inst. Mech. Engrs* **17**, 55–65.

Rees, D. W. A. (1987a). An experimental appraisal of equi-plastic strain multi-surface hardening model. *Acta Mech.* **70**, 193–219.

Rees, D. W. A. (1987b). Application of classical plasticity theory to non-radial loading paths. *Proc. Roy. Soc. Lond.* **A410**, 443–475.